BIOCHEMISTRY
including biophysical chemistry & molecular biology

Article

pubs.acs.org/biochemistry

The Cys-Tyr Cross-Link of Cysteine Dioxygenase Changes the Optimal pH of the Reaction without a Structural Change

Casey G. Davies,[†] Matthias Fellner,[†] Egor P. Tchesnokov,[†] Sigurd M. Wilbanks,[‡] and Guy N. L. Jameson*,[†]

[†]Department of Chemistry and MacDiarmid Institute for Advanced Materials and Nanotechnology and [‡]Department of Biochemistry, University of Otago, P.O. Box 56, Dunedin 9054, New Zealand

ABSTRACT: Cysteine dioxygenase (CDO) is a non-heme monoiron enzyme with an unusual posttranslational modification in the proximity of the ferrous iron active site. This modification, a cysteine to tyrosine thioether bond, cross-links two β-strands of the β-barrel. We have investigated its role in catalysis through a combined crystallographic and kinetic approach. The C93G variant lacks the cross-link and shows little change in structure from that of the wild type, suggesting that the cross-link does not stabilize an otherwise unfavorable conformation. A pH-dependent kinetic study shows that both cross-linked and un-cross-linked CDO are active but the optimal pH decreases with the presence of the cross-link. This result reflects the effect of the thioether bond on the pK_a of Y157 and this residue's role in catalysis. At higher pH values, k_{cat} is also higher for the cross-linked form, extending the pH range of activity. We therefore propose that the cross-link also increases activity by controlling deleterious interactions involving the thiol/ate of C93.

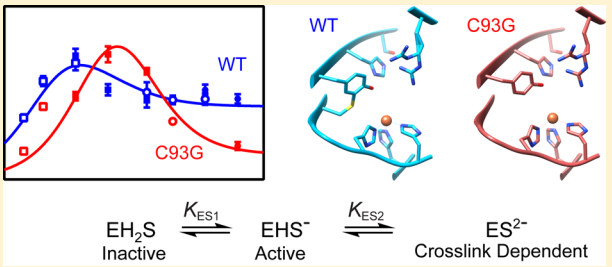

Cysteine dioxygenase (CDO) is a non-heme monoiron enzyme that has attracted interest because of its primary role in the oxidative breakdown of cysteine and also because of its unusual structural characteristics.[1−3] These characteristics include a neutral ligand coordination site for ferrous iron provided by three histidine residues and a posttranslational modification consisting of a cysteine−tyrosine thioether bond.[4−7] It has been proposed by us and others that both these structural motifs are vital for explaining enzymatic activity.[6,8−13]

In a previous study, we showed that iron is tightly bound to the three histidines with a dissociation constant (6 μM)[14] that is comparable with that of the anionic His_2/CO_2^- ligand set used by most other non-heme monoiron enzymes. We further showed through Mössbauer spectroscopy that the ferrous iron is octahedrally coordinated in the resting state and undergoes a reduction in coordination number upon cysteine binding.[14] This is consistent with independent spectroscopic and binding studies that showed that iron binding is not changed but substrate binding is by the unusual choice of ligands for the first coordination sphere.[15−17]

The cysteine−tyrosine cross-link of mammalian CDO is present in only ∼50% of either recombinant protein or cell lysate.[8−10] Dominy et al. and our group showed that cross-link formation required CDO-bound iron and the presence of substrates dioxygen and cysteine.[7,8,10] The proportion of cross-link can be reduced by excluding oxygen during expression and purification or increased through catalytic cycling.[8] The initial rate of catalytic turnover was seen to increase with the amount of cross-link present, and more recently, it has been suggested that both k_{cat} and K_M are altered.[8,9] Indeed, site-directed mutagenesis to substitute C93 with alanine or serine reduces activity, suggesting that the cross-link plays an important role in catalysis.[6,9−13]

However, Dominy et al. purified and characterized four bacterial CDOs that show substantial activity in the absence of a cross-link. Sequence alignment shows that those bacterial CDOs possess glycine rather than cysteine at the position equivalent to C93 yet nonetheless show activity similar to those of mammalian CDOs.[18] There are two crystal structures of proposed bacterial CDOs [Protein Data Bank (PDB) entries 2GM6 and 3USS], and in both cases, there does not appear to be gross rearrangement of the active site with the tyrosine occupying a very similar position relative to the iron. The structure and high activity of the bacterial CDOs suggest that a C93G variant would complement the C93A and C93S variants used by others to probe the role of the cysteine−tyrosine cross-link.

The cysteine−tyrosine cross-link is known from model chemistry to affect both the redox potential and the pK_a of the tyrosine, decreasing both.[19] It is therefore important that the kinetic parameters used to investigate the role of the cross-link are measured over a pH range. In this study, we have therefore determined the crystal structure of the C93G CDO variant (PDB entry 4UBG) and conducted a complete pH kinetic profile of CDO with different proportions of the cross-link and compared them with those of the C93G variant.

Received: October 12, 2014
Revised: November 8, 2014
Published: November 12, 2014

   dx.doi.org/10.1021/bi501277a | *Biochemistry* 2014, 53, 7961−7968

MATERIALS AND METHODS

Expression and Purification of 60% Cross-Linked Wild-Type (WT) CDO. Expression and purification of *Rattus norvegicus* CDO using Strep-Tag affinity technology were performed as described previously.[14] Purified protein was found to be a least 95% pure by sodium dodecyl sulfate−polyacrylamide gel electrophoresis (SDS−PAGE) analysis (Figure 1A). Purified protein was extensively dialyzed (dilution factor of $>10^9$) against 20 mM TRIS-HCl buffer (pH 8.0) containing 40 mM NaCl. Dialyzed protein was concentrated (>700 μM) and found to contain ∼15% endogenously bound iron as previously reported.[14]

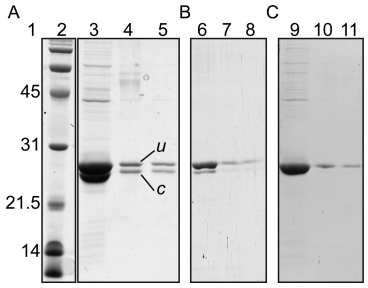

Figure 1. SDS−PAGE analysis of purified WT and C93G rat CDO produced using different expression conditions. Purified samples of rat CDO were resolved by SDS−PAGE on a 15% (w/v) polyacrylamide gel and detected by staining with Coomassie Blue. (A) WT CDO produced using standard expression conditions: lane 1, molecular weights (MWs, kDa) of selected markers; lane 2, migration pattern of MW markers; lane 3, purified protein sample; lanes 4 and 5, 20- and 40-fold diluted samples, respectively, shown to illustrate sample purity. Symbols *u* and *c* indicate the mobility of un-cross-linked and cross-linked CDO, respectively. (B) WT CDO produced using auto-induction expression media: lane 6, purified protein sample; lanes 7 and 8, 20- and 40-fold diluted samples, respectively. (C) C93G variant produced using standard expression conditions: lane 9, purified C93G variant sample; lanes 10 and 11, 20- and 40-fold diluted samples, respectively.

Expression and Purification of WT CDO Depleted of the Cross-Link (20%). Mainly un-cross-linked WT CDO was produced and processed in exactly the same way as 60% cross-linked WT CDO except that autoinduction medium (For-medium) was used during protein expression according to the manufacturer's protocol. Figure 1B illustrates an approximately 13% cross-linked purified WT CDO.

Expression and Purification of the *R. norvegicus* C93G CDO Variant. The cysteine 93 to glycine (C93G) mutation was generated using primers (Invitrogen) containing a TGC-to-GGC codon substitution. A polymerase chain reaction catalyzed by *PfuUltra* High-Fidelity DNA polymerase (Stratagene, Agilent Technologies) was conducted according to the manufacturer's protocol. Both strands of the CDO coding region of the expression construct (pPR-IBA1/CDO/C93G) were fully sequenced to confirm the absence of adventitious mutations (Genetic Analysis Services at the University of Otago). Expression and purification conditions were the same as for 60% cross-linked WT CDO. As expected, CDO with the C93G substitution resolved into one band upon being subjected to SDS−PAGE, illustrating the absence of the posttranslational modification associated with C93−Y157 in WT CDO (Figure 1C).

Iron Reconstitution of the CDO Active Site. The CDO active site was reconstituted with ferrous iron through addition of ∼0.95 equiv of ferrous ammonium sulfate. The sample was subjected to treatment with analytical grade Chelex 100 sodium form, 200−400 mesh (Bio-Rad), to remove any unbound iron.[14] After such treatment, protein preparations of WT and C93G CDO equally contained ∼0.95 equiv of iron as judged by a colorimetric assay using ferrozine.[14,20,21] This observation suggested that neither the minimization of cross-linked CDO nor its complete absence (C93G variant) compromised the quality of binding of iron to the CDO active site.

Crystallization and Structural Determination of the C93G Variant. Crystals were grown and processed using the same conditions described previously.[22] Hanging drops of 1.5 μL of approximately 7 mg/mL C93G CDO [10 mM sodium phosphate and 20 mM NaCl (pH 7.5)] and 0.6 μL of crushed WT CDO seeds in their own growth solution [25% (w/v) polyethylene glycol 1500, 13 mM succinate, 44 mM sodium phosphate, and 44 mM glycine (pH 5.2)] and 1.5 μL of reservoir buffer were allowed to equilibrate above the reservoir buffer [26% (w/v) polyethylene glycol 4000, 200 mM ammonium acetate, and 100 mM sodium citrate (pH 6.3)]. Data were collected at the MX2 beamline of the Australian Synchrotron. Using 1° oscillations, 180° of data were collected on an ADSC (Area Detector Systems Corp.) detector with a detector distance of 180 mm at 13000 eV, 80% attenuation, and 5 s exposure. Data were indexed in space group $P4_32_12$, with unit cell dimensions of 57.84, 57.84, and 122.7 Å, and integrated in iMosflm. Exclusion of data near ice rings decreased the completeness in certain shells.[23] Scaling was done using Aimless;[24] 5% of reflections were reserved for the calculation of R_{free} (Table 1). The resolution was initially cut back to 1.82 Å based on the $CC_{1/2}$ values of >0.5[25] reported by Phenix. PDB entry 4KWJ[22] was used for molecular replacement in Phenix.Phaser[26] with one monomer in the asymmetric unit. The active site iron and sodium solvent molecules were placed using Phaser-EP[26] (MR-SAD). Phenix.Refine,[26] Phenix.Ready-set,[26] and COOT[27] were used for refinement; in later refinement steps, the resolution was cut to 1.90 Å to improve the quality of the data. Translation/libration/screw (TLS) analysis[28] was used as implemented in the TLSMD Web server.[29] Coordinates and structure factors were deposited in the Protein Data Base as entry 4UBG.

Choice of Buffers for pH Studies. To check for buffer-induced artifacts, kinetic experiments were repeated at certain pH values using alternative buffers. We found that tricine buffer had a significant inhibitory effect on cysteine dioxygenation when compared to those of TRIS and/or CHES buffers at the same pH. This buffer effect has been previously reported in the context of alkaline phosphatase.[30] Because all the kinetic experiments were conducted at the same temperature (22 °C), usage of TRIS buffer was justified. The following buffers were used for the pH study: MES, MOPS, TRIS, and CHES. To ensure that the pH of the reaction mixture remained constant under reaction conditions involving initial cysteine concentrations of up to 40 mM, we used buffers at a concentration of 200 mM. Particular care was taken to ensure that the ionic strength of the buffers remained the same across the pH profile (150 mM) by addition of NaCl.

Measurement of CDO Activity. CDO activity was measured using a 96-well plate Ellman's assay as previously reported.[31] An experimental grid consisting of at least 10 points for time courses at five different cysteine substrate concen-

dx.doi.org/10.1021/bi501277a | *Biochemistry* 2014, 53, 7961−7968

Table 1. X-ray Data Collection, Reduction, and Crystallographic Refinement Statistics of C93G Resting State 4UBG

resolution range	52.32−1.82 Å (1.86−1.82 Å)[a]
no. of observed reflections	232626 (14581)
no. of unique reflections	17317 (1131)
redundancy	13.4 (12.9)
completeness	88.3% (100.0%)
I/σ	16.8 (1.9)
$CC_{1/2}$	0.892 (0.719)
R_{merge}[b]	0.127 (1.246)
resolution range used in the final refinement	42.10−1.90 Å (1.97−1.90 Å)
$CC_{1/2}$	0.876 (0.855)
R_{merge}[b]	0.114 (0.601)
no. of reflections used in the refinement	27858 (1488)
R_{cryst}[c]	0.202 (0.373)
R_{free}[d]	0.241 (0.418)
Ramachandran outliers[e]	0%
Ramachandran unfavorable[e]	1.1%
Ramachandran favorable[e]	98.9%
rotamer outliers[e]	0.6%
Clashscore[e]	7.82
deviation from ideal bond lengths	0.008 Å
deviation from ideal bond angles	1.055°
average *B* factor	22.22 Å^2

[a]Values in parentheses indicate the highest-resolution shell. [b]$R_{merge} = \sum|I_{obs} - I_{ave}|/\sum I_{ave}$. [c]$R_{cryst} = \sum|F_{obs} - F_{calc}|/\sum F_{obs}$ computed over a working set composed of 95% of the data. [d]$R_{free} = \sum|F_{obs} - F_{calc}|/\sum F_{obs}$ computed over a test set composed of 5% of the data. [e]Calculated using Molprobity.

trations was used to determine each set of k_{cat} and K_M values. All kinetic data were analyzed using Microsoft Office Excel and Graph Pad Prism (6.0).

Modeling the pH Dependence of Cysteine Dioxygenation. To a first approximation, it is valid to treat an enzyme as having two dissociable groups in the active site with only the singly protonated form proceeding through catalysis. This translates into a pH profile resembling a bell shape or normal distribution curve. To account for the pH profile observed for WT CDO with 60% cross-link (Figure 4; k_{cat} remains constant and is only marginally reduced at higher pH), we therefore added a second catalytically active ES species to Scheme 1. The

Scheme 1. Enzyme Reaction Used To Model the pH Profile

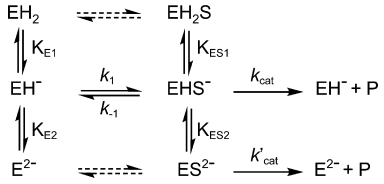

molecular dissociation constants K_{E1} and K_{E2} describe the first and second proton dissociations, respectively. K_{ES1} and K_{ES2} represent the first and second proton dissociations, respectively, of the enzyme−substrate species. k_{cat} represents the summation of all rates after the formation of ES species and dissociation of the product. For simplification, this scheme deals only with the rapid equilibrium of the substrate and hydrogen binding. k_1 and k_{-1} represent the equilibrium constants for the dotted lines as well as the solid line equilibrium arrows between EH^- and EHS^-.

By deriving the molecular dissociation constants from the group dissociation constants, under steady state conditions, we can apply the following equation[32,33]

$$k_{cat} = u\left[\frac{\acute{k}_{u,cat} + \acute{k}'_{u,cat}\left(\frac{K_{u,ES2}}{[H^+]}\right)}{\frac{[H^+]}{K_{u,ES1}} + 1 + \frac{K_{u,ES2}}{[H^+]}}\right] + c\left[\frac{\acute{k}_{c,cat} + \acute{k}'_{c,cat}\left(\frac{K_{c,ES2}}{[H^+]}\right)}{\frac{[H^+]}{K_{c,ES1}} + 1 + \frac{K_{c,ES2}}{[H^+]}}\right] \quad (1)$$

where k_{cat} is the catalytic constant for the formation of the product from the enzyme substrate species, $\acute{k}_{cat}$ is the pH-corrected parameter,[34] and K_{ES} describes the molecular dissociation constants for the enzyme substrate complex. u and c represent the proportion of un-cross-linked and cross-linked CDO, respectively.

Determination of Comparative Efficiency of Cysteine Dioxygenation. On the basis of recent interpretation[35−38] of the Michaelis−Menten catalytic efficiency (specificity constant), eq 2 was used to calculate the efficiency of cysteine dioxygenation by WT and C93G CDO

$$E_F = \frac{k_{cat}}{k_{dif}(K_M + [S])} \times 10^{10} \quad (2)$$

where E_F is the efficiency constant and k_{dif} is the rate of diffusion that is estimated[39] to be $\sim 10^9$ M^{-1} s^{-1}. The comparative efficiency of cysteine dioxygenation was determined by subtracting the pH profile of catalytic efficiency of C93G from the respective profile of WT CDO.

RESULTS

Expression and Purification of WT CDO and Its C93G Variant. We have previously produced CDO with low proportions of cross-link by using anaerobic expression conditions.[8] In a recent study by Njeri et al., the un-cross-linked WT CDO has been produced using a metal chelator added prior to the induction of protein expression.[13] In this study, we employed standard and autoinduction expression media to produce different proportions of cross-linked CDO active sites (Figure 1A,B). The fraction of cross-link can be determined through densitometry of isoforms separated by SDS−PAGE. The cross-linked state of the upper and lower bands has been confirmed previously by mass spectrometry.[7] Representative SDS−PAGE gels shown in panels A and B of Figure 1 were found to contain 42 ± 10 and 13 ± 5% cross-link, respectively. This observation is consistent with previous accounts of CDO expression.[8,9] Unexpectedly, after dialysis, concentration, and active site iron reconstitution, we observed an increase in the proportion of the cross-linked CDO present in the purified protein samples (59 ± 10 and 21 ± 5% for CDO expressed under standard and autoinduction expression conditions, respectively). Such an increase in the cross-linked fraction has not been reported previously. However, in a recent study by Njeri et al., they reported a cross-link in iron-free CDO active sites, highlighting the fact that little is known about the actual mechanism of cross-link formation.[13] The purified protein preparations of the C93G CDO variant migrated as a

dx.doi.org/10.1021/bi501277a | Biochemistry 2014, 53, 7961−7968

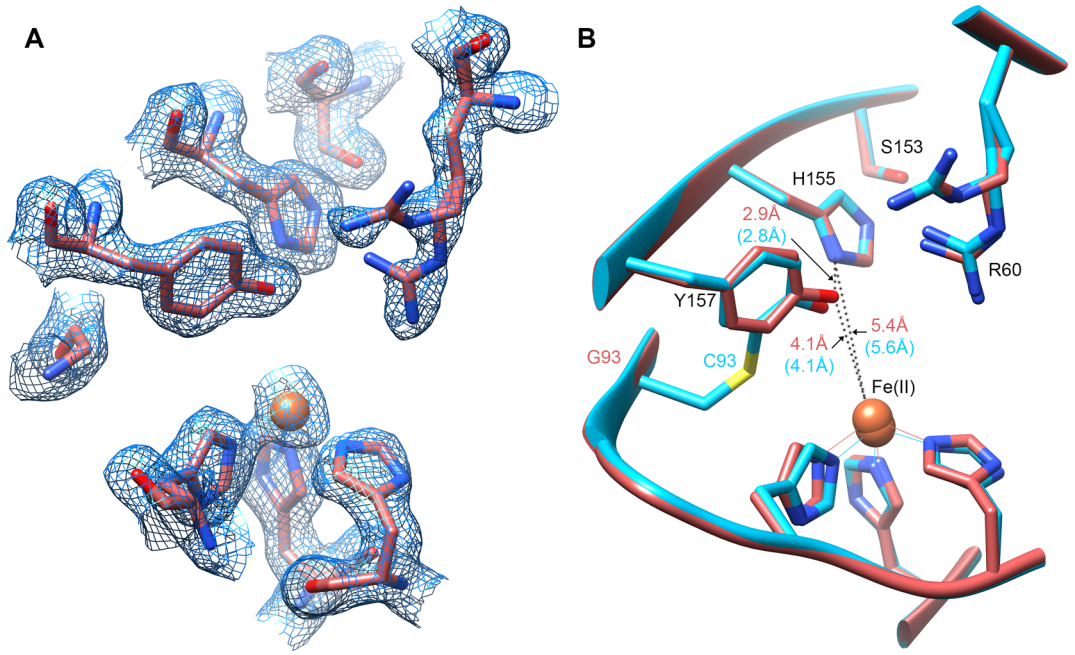

Figure 2. Crystal structure of the C93G CDO variant. Selected conserved side chains are shown with oxygen, nitrogen, sulfur, and iron atoms colored bright red, blue, yellow, and orange, respectively. (A) Active site residues of the C93G CDO variant. Shown is the $2mF_o - DF_c$ active site electron density (contoured at 1.2σ) and the refined model. (B) Structural comparison of the C93G CDO variant (PDB entry 4UBG, main chain cartoon and side chain carbon atoms colored dull red) superimposed on WT CDO (PDB entry 4KWJ, cyan) using a Cα atom alignment. Values in red indicate interatomic distances for the iron, tyrosine hydroxyl, and imidazole nitrogen of 4UBG; cyan values in parentheses give the corresponding distances in WT CDO (4KWJ).

single band when they were subjected to SDS−PAGE, which is consistent with ablation of the cross-link (Figure 1C).

Structural Consequences of Cross-Link Ablation. Crystallographic data support an atomic-resolution structure of the C93G variant (PDB entry 4UBG) and confirm the lack of any cross-link to Y157 (Figure 2A). The superposition of the crystal structures of the C93G variant (PDB entry 4UBG) and WT CDO (PDB entry 4KWJ) is shown in Figure 2B. On the basis of 187 Cα atom pairs, the root-mean-square deviation for this superposition[40] is 0.164 Å. Overall, no major structural changes can be observed as a result of the absence of the cross-link. The C93G variant active site is organized in the same manner as its wild-type counterpart, and the absence of the cross-link has no effect on the positioning of the Y157 side chain. In both structures, the hydroxyl-group of Y157 is 4.1 Å from the active site iron. Importantly, the respective interatomic distances are also conserved within the hydrogen bonding network of the highly conserved S153-H155-Y157 triad. The two conformations of R60 observed in the crystal structure of WT CDO (PDB entry 4KWJ) are also present in the C93G variant, further illustrating structural similarities between the active sites of the variant and native enzyme. As in other CDO structures, high *B* factors are observed in the loop including residue 113, and TLS analysis isolates this region (residues 111−127) as a segment of elevated, but not striking, mobility (translation of ∼0.9 Å). TLS analysis of WT CDO (PDB entry 4WKJ) shows correlated motions of segments that are strands of the β-barrel and are cross-linked via C93−Y157 (residues 11−110 and 128−169). TLS analysis of C93G shows greater movement of residues 128−169 (compared to that of WT) but less movement of residues 11−110, leading to reduced correlation of movement of the two segments in the C93G mutant. However, no significant domain movements become evident.

Kinetic Studies of the pH Dependence of Cysteine Dioxygenation. The initial rate of cysteine oxidation was measured using a high-throughput 96-well plate spectrophotometric Ellman's assay as previously established in our laboratory.[31] The correlation between the rate of cysteine substrate disappearance and the rate of CSA product formation under the assay conditions was confirmed for both the WT and C93G variant CDO preparations used in this study through HPLC−ELSD analysis as previously established in our laboratory.[41] The initial velocities of cysteine depletion determined by Ellman's reagent were normalized to the active site iron concentration and plotted versus the cysteine substrate concentration (Figure 3). The data were fit with the Michaelis−Menten kinetic parameters, k_{cat} and K_M (Table 2). The steady state activity of CDO protein preparations with various proportions of cross-link was subject to a pH effect. Therefore, a pH profile from pH 5.8 to 9.1 was determined for WT and C93G variant CDO.

The k_{cat}−pH profile for WT CDO containing 60% cross-linked active sites has an optimal pH of 6.6 (Figure 4). This value is within the range (6.1−9.5) of previously reported optimal pH values for WT CDO.[9,42−49] However, in striking difference to previous studies at higher pH values, the value of k_{cat} decreased only marginally and remained independent of further increases in pH. This unusual pattern of a pH profile was also observed for k_{cat} of WT CDO containing 20% cross-linked active sites; however, in this case, the optimal pH shifted to ∼7.3 and activity was lower. Consistent with our previous report,[8] throughout the pH profile, an ∼3-fold increase in the proportion of cross-linked WT CDO active sites correlated with an ∼2.3-fold increase in k_{cat}. Other studies reported

dx.doi.org/10.1021/bi501277a | *Biochemistry* 2014, 53, 7961−7968

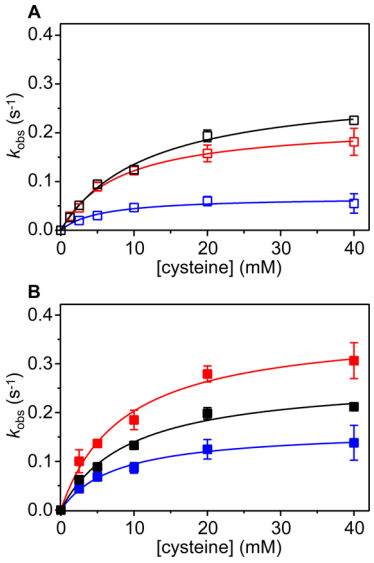

Figure 3. Typical data analysis used for the determination of the steady state Michaelis–Menten parameters for the cysteine dioxygenation reaction catalyzed by WT CDO containing 60% (black) and 20% (blue) cross-link and by the C93G CDO variant containing 0% (red) cross-link measured at pH 6.6 (A) and pH 7.1 (B). Data points were fit to the Michaelis–Menten equation, and the parameters were calculated used GraphPad Prism 6.0. The full set of parameters can be found in Table 2. Error bars represent the standard deviation of at least three data points.

Table 2. Michaelis–Menten Parameters for Cysteine Dioxygenation Determined at Various pH Values

pH	k_{cat} (s^{-1})	K_M (mM)	k_{cat}/K_M (M^{-1} s^{-1})
	60% Cross-Linked WT CDO		
5.8	0.19 ± 0.01	16 ± 2	12 ± 3
6.1	0.30 ± 0.01	12 ± 2	25 ± 5
6.6[a]	0.36 ± 0.02	10 ± 2	37 ± 9
7.1	0.27 ± 0.02	9 ± 2	29 ± 7
7.7[a]	0.25 ± 0.03	5 ± 1	56 ± 20
8.1	0.24 ± 0.01	6 ± 1	42 ± 10
8.6[a]	0.26 ± 0.02	5 ± 1	52 ± 20
9.1	0.24 ± 0.01	5 ± 1	49 ± 20
	20% Cross-Linked WT CDO		
5.8	0.06 ± 0.01	10 ± 4	6 ± 4
6.1	0.07 ± 0.01	5 ± 2	13 ± 8
6.6	0.10 ± 0.01	17 ± 2	6 ± 1
7.1	0.17 ± 0.01	8 ± 1	22 ± 4
8.1	0.11 ± 0.01	3 ± 1	36 ± 10
9.1	0.12 ± 0.01	2 ± 1	56 ± 30
	0% Cross-Linked C93G CDO Variant		
5.8	0.09 ± 0.01	7 ± 2	12 ± 4
6.1	0.22 ± 0.01	8 ± 1	28 ± 3
6.6	0.25 ± 0.01	37 ± 3	7 ± 1
7.1	0.38 ± 0.02	9 ± 2	44 ± 20
7.7	0.33 ± 0.01	3 ± 1	95 ± 20
8.1	0.16 ± 0.01	2 ± 1	81 ± 30
9.1	0.10 ± 0.01	2 ± 1	46 ± 30

[a]Average of two buffers measured at the same pH.

greater increases in CDO activity as a function of the fraction of cross-linked CDO active sites.[9,13] However, the most recent study of human CDO by Arjune et al. did not observe any

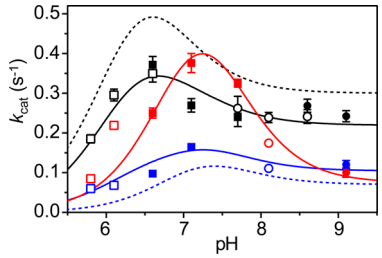

Figure 4. k_{cat}–pH profile of cysteine dioxygenation by WT CDO containing 60% (black) and 20% (blue) cross-link and by the C93G CDO variant containing 0% (red) cross-link. Empty squares represent data collected in the presence of 200 mM MOPS buffer, filled squares those in MES, empty circles those in TRIS, and filled circles those in CHES. Error bars represent the standard deviation of at least three data points. Lines represent fits to eq 1. The dashed lines show the theoretical profile of 100% cross-linked (black) and 0% cross-linked (blue) forms.

effect of the cross-linked fraction of the active sites on the Michaelis–Menten parameters.[12]

The k_{cat}–pH profile for the C93G CDO variant containing 0% cross-linked active sites illustrates an optimal pH of ∼7.3 reminiscent of the optimal pH observed for WT CDO containing 20% cross-linked active sites. However, the C93G k_{cat} is consistently and significantly higher than the corresponding value for the 20% cross-linked WT CDO across most of the pH spectrum. The C93G CDO variant k_{cat}–pH profile also differs from that of WT CDO containing 60% cross-linked active sites. The optimal pH differs, and the C93G CDO variant k_{cat} is higher at pH 7 and lower elsewhere. Interestingly, the C93G variant presented here shows activity across all pH values, and its k_{cat} is indistinguishable from that of WT, if compared at the respective pH optima.

Reinterpretation[35−38] of the Michaelis–Menten catalytic efficiency (specificity constant) suggested that for a study of multiple enzymes (20 and 60% cross-linked WT and 0% cross-linked C93G variant CDO) with the same set of substrates (cysteine and oxygen) the commonly used parameter k_{cat}/K_M is not appropriate. Therefore, in this study, this metric was not employed for comparative analysis. Instead, eq 2 was used for comparison. This approach integrates values of k_{cat}, K_M, and substrate concentration.

DISCUSSION

Posttranslational modifications can alter protein levels or activity, and as such, they are relevant to cellular homeostasis. Fractional formation of the autocatalytic thioether bond (cross-link) in the active site of mammalian CDO has been thought to have a regulatory role in cysteine dioxygenation through activation of enzymatic activity. The mechanism of such activation remains unknown. Previous experimental studies assessed changes in the Michaelis–Menten kinetic parameters associated with an increase in the fraction of cross-linked WT CDO or cross-link ablation in C93A and C93S CDO variants, with data generally collected at the optimal pH for cross-linked CDO. While patterns of apparent enzymatic activation have been observed, the cross-study analysis of those patterns is difficult because of the spread of optimal pH values for WT CDO and the absence of such for the variants. In this study, we present evidence that the removal of the posttranslational modification from the CDO active site has no obvious structural consequences. We report a deviation of the CDO

dx.doi.org/10.1021/bi501277a | Biochemistry 2014, 53, 7961−7968

WT pH profile from the typical bell-shaped curve and present a theoretical model for rationalizing this observation.

The comparative efficiency of cysteine dioxygenation extracted from integrative analysis of CDO WT and C93G variant pH profiles argues that removal of the cross-link does not translate into a dramatic reduction in enzymatic efficiency, and the C93G variant is more efficient at neutral pH (Figure 5).

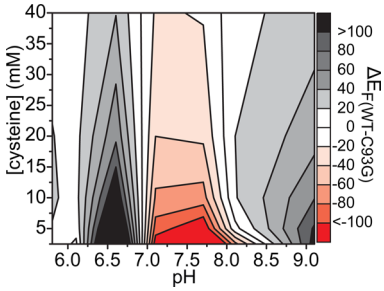

Figure 5. Comparative efficiency (ΔE_F) of cysteine dioxygenation using the theory of perfect catalysis under steady state conditions. The color scheme represents the more efficient species at any given pH. Black and red contours represent the greater efficiency of WT CDO (60% cross-link) and C93G CDO (0% cross-link), respectively. The details of data analysis used to generate this figure are described in Materials and Methods.

Previous studies have substituted C93 with alanine or serine, but in all these studies, kinetic data have been collected at only one pH; therefore, the data are difficult to compare to each other and to the current investigation.[6,9−13] However, all previous studies show a decrease in k_{cat}/K_M compared to that of WT. In contrast, C93G shows k_{cat}/K_M values comparable to that of WT over all pH values (Table 2). The robust catalytic activity of C93G therefore suggests that steric clashes and/or hydrogen bonding interactions between alanine/serine and the iron−substrate complex explain the lower reactivity of these variants. Overall, the k_{cat}−pH profile for the C93G CDO variant is consistent with the observation that some bacterial CDO enzymes containing glycine at the C93-relevant position are as active as their mammalian counterparts.[18]

We present the first structure of an un-cross-linked mammalian CDO. All previous structures report that CDO in the crystal is entirely or predominantly cross-linked, independent of the cross-link fraction of CDO in the crystallization solution. The structure of C93G reported here demonstrates that the un-cross-linked form is competent to crystallize and indeed is structurally almost indistinguishable from the cross-linked version. This strongly suggests that the cross-link does not play a crucial structural role in active site organization of CDO. TLS analysis suggests that the segment surrounding Y157 is less mobile when cross-linked, but the overall change in mobility is not striking. The modest change in mobility may account for the selective crystallization of cross-linked protein when both cross-linked and un-cross-linked forms are present.

To investigate whether the cross-link affects the pK_a of the highly conserved Y157, we collected a pH profile for both WT and C93G. Fitting of k_{cat} as a function of pH using eq 1 for WT CDO with different proportions of cross-link showed that both cross-linked and un-cross-linked CDO were active with different parameters (Table 3). Theoretical pH profiles for 100 and 0% cross-linked CDO are presented as dashed lines in Figure 4. Comparison of the profile of C93G, which is unable to form the cross-link, with the theoretical profile of 0% cross-linked CDO shows the shape of the pH dependence is identical with the same pK values and pH optima. However, k_{cat} is significantly higher for C93G compared to 0% cross-link at nearly every pH, showing that although the same proton acceptors and donors are used in both proteins, free C93 must be reducing activity. The mechanism by which this occurs, e.g. a steric interaction, is not yet known. Importantly, however, the pH optima of k_{cat} decreased from fully un-cross-linked to fully cross-linked, and this corresponds with a downshift of the pK values calculated by the fit of approximately 1 pH unit. Altogether, this supports the role of the cross-link in reducing the pK_a of Y157 as suggested by model chemistry and further indicates the importance of Y157 in the catalytic cycle.

Table 3. pH-Dependent Parameters Derived from eq 1

	cross-linked	un-cross-linked	C93G
$\acute{k}_{cat}$ (s^{-1})	0.8	0.2	0.8
$\acute{k}'_{cat}$ (s^{-1})	0.3	0.07	0.05
pK_{ES1}	6.1	7.0	7.0
pK_{ES2}	6.7	7.5	7.5

C93G showed a more typical bell-shaped curve with a pH optimum of 7.3, but WT showed considerable activity at high pH. This deviation was consistent with an additional, active, doubly deprotonated enzyme−substrate complex (see Scheme 1). This is intriguing as it suggests that C93 has a significant deleterious effect on catalysis distinct from its role in forming the cross-link. We therefore postulate a protective role of the thioether bond in the CDO active site: cross-link formation removes labile thiol from the active site of CDO and expands the active pH range. We propose that the ability of the cross-link to preserve activity at high pH reflects suppression of a competing interaction rather than a direct contribution to cysteine dioxygenation. The thiolate of deprotonated C93 would sit close to the binding sites of dioxygen and substrate cysteine and could produce unwanted interactions in the active site. Alternatively, a C93 thiolate may attack the substrate cysteine competing with the dioxygenation reaction. Possible products of this reaction include formation of cystine either as a modification of C93 as seen for C164[7] or as an alternative, diffusible oxidation product. Cross-link formation would abolish this competing reaction. This interpretation explains our kinetic data and much of that of other researchers but begs the question of why C93 has been conserved among mammalian CDOs, especially because the protein is not fully cross-linked under physiological conditions.

Although reductions of the pK_a and reduction potential of Y157 remain potential benefits of the cross-link, it is not clear that a greater pH range is sufficient to support the conservation of C93. Comparison of the catalytic efficiency shows that over a quite large physiological cysteine concentration range (<5 mM) and pH range removal of the cross-link via the C93G mutation leads to a considerably more efficient dioxygenation reaction. Indeed, an active site thiolate is avoided in bacterial CDOs by genetic substitution of a glycine for this cysteine. If C93G contributes to the regulation of mammalian CDO, the mechanism depends more on inhibition of competing reactions catalyzed by the free thiol of C93 than on the greater reactivity of cross-linked Y157.

dx.doi.org/10.1021/bi501277a | *Biochemistry* 2014, 53, 7961−7968

AUTHOR INFORMATION

Corresponding Author

*Department of Chemistry, University of Otago, P.O. Box 56, Dunedin 9054, New Zealand. Telephone: +64 3 479 8028. E-mail: gjameson@chemistry.otago.ac.nz.

Funding

This work was supported by the Marsden Fund of the Royal Society of New Zealand (G.N.L.J., PI; S.M.W., AI). E.P.T. was supported by a Canadian Institutes of Health Research Postdoctoral Fellowship.

Notes

The authors declare no competing financial interest.

REFERENCES

(1) Stipanuk, M., Simmons, C., Andrew Karplus, P., and Dominy, J., Jr. (2011) Thiol dioxygenases: Unique families of cupin proteins. *Amino Acids 41*, 91−102.

(2) Aluri, S., and de Visser, S. P. (2007) The mechanism of cysteine oxygenation by cysteine dioxygenase enzymes. *J. Am. Chem. Soc. 129*, 14846−14847.

(3) Kumar, D., Thiel, W., and de Visser, S. P. (2011) Theoretical study on the mechanism of the oxygen activation process in cysteine dioxygenase enzymes. *J. Am. Chem. Soc. 133*, 3869−3882.

(4) McCoy, J. G., Bailey, L. J., Bitto, E., Bingman, C. A., Aceti, D. J., Fox, B. G., and Phillips, G. N. (2006) Structure and mechanism of mouse cysteine dioxygenase. *Proc. Natl. Acad. Sci. U.S.A. 103*, 3084−3089.

(5) Simmons, C. R., Liu, Q., Huang, Q., Hao, Q., Begley, T. P., Karplus, P. A., and Stipanuk, M. H. (2006) Crystal structure of mammalian cysteine dioxygenase: A novel mononuclear iron center for cysteine thiol oxidation. *J. Biol. Chem. 281*, 18723−18733.

(6) Ye, S., Wu, X. A., Wei, L., Tang, D., Sun, P., Bartlam, M., and Rao, Z. (2007) An insight into the mechanism of human cysteine dioxygenase: Key roles of the thioether-bonded tyrosine-cysteine cofactor. *J. Biol. Chem. 282*, 3391−3402.

(7) Kleffmann, T., Jongkees, S. K., Fairweather, G., Wilbanks, S., and Jameson, G. L. (2009) Mass-spectrometric characterization of two posttranslational modifications of cysteine dioxygenase. *JBIC, J. Biol. Inorg. Chem. 14*, 913−921.

(8) Siakkou, E., Rutledge, M. T., Wilbanks, S. M., and Jameson, G. N. L. (2011) Correlating crosslink formation with enzymatic activity in cysteine dioxygenase. *Biochim. Biophys. Acta 1814*, 2003−2009.

(9) Li, W., Blaesi, E. J., Pecore, M. D., Crowell, J. K., and Pierce, B. S. (2013) Second-Sphere Interactions between the C93−Y157 Cross-Link and the Substrate-Bound Fe Site Influence the O_2 Coupling Efficiency in Mouse Cysteine Dioxygenase. *Biochemistry 52*, 9104−9119.

(10) Dominy, J. E., Hwang, J., Guo, S., Hirschberger, L. L., Zhang, S., and Stipanuk, M. H. (2008) Synthesis of Amino Acid Cofactor in Cysteine Dioxygenase Is Regulated by Substrate and Represents a Novel Post-translational Regulation of Activity. *J. Biol. Chem. 283*, 12188−12201.

(11) Joseph, C. A., and Maroney, M. J. (2007) Cysteine dioxygenase: Structure and mechanism. *Chem. Commun. 28*, 3338−3349.

(12) Arjune, S., Schwarz, G., and Belaidi, A. (2014) Involvement of the Cys-Tyr cofactor on iron binding in the active site of human cysteine dioxygenase. *Amino Acids*, 1−9.

(13) Njeri, C. W., and Ellis, H. R. (2014) Shifting redox states of the iron center partitions CDO between crosslink formation or cysteine oxidation. *Arch. Biochem. Biophys. 558*, 61−69.

(14) Tchesnokov, E. P., Wilbanks, S. M., and Jameson, G. N. L. (2012) A Strongly Bound High-Spin Iron(II) Coordinates Cysteine and Homocysteine in Cysteine Dioxygenase. *Biochemistry 51*, 257−264.

(15) Leitgeb, S., Straganz, G. D., and Nidetzky, B. (2009) Biochemical characterization and mutational analysis of the mononuclear non-haem Fe^{2+} site in Dke1, a cupin-type dioxygenase from *Acinetobacter johnsonii*. *Biochem. J. 418*, 403−411.

(16) Diebold, A. R., Neidig, M. L., Moran, G. R., Straganz, G. D., and Solomon, E. I. (2010) The Three-His Triad in Dke1: Comparisons to the Classical Facial Triad. *Biochemistry 49*, 6945−6952.

(17) Diebold, A. R., Straganz, G. D., and Solomon, E. I. (2011) Spectroscopic and Computational Studies of α-Keto Acid Binding to Dke1: Understanding the Role of the Facial Triad and the Reactivity of β-Diketones. *J. Am. Chem. Soc. 133*, 15979−15991.

(18) Dominy, J. E., Simmons, C. R., Karplus, P. A., Gehring, A. M., and Stipanuk, M. H. (2006) Identification and Characterization of Bacterial Cysteine Dioxygenases: A New Route of Cysteine Degradation for Eubacteria. *J. Bacteriol. 188*, 5561−5569.

(19) Itoh, S., Takayama, S., Arakawa, R., Furuta, A., Komatsu, M., Ishida, A., Takamuku, S., and Fukuzumi, S. (1997) Active Site Models for Galactose Oxidase. Electronic Effect of the Thioether Group in the Novel Organic Cofactor. *Inorg. Chem. 36*, 1407−1416.

(20) Stookey, L. L. (1970) Ferrozine: A new spectrophotometric reagent for iron. *Anal. Chem. 42*, 779−781.

(21) Pierce, B. S., Gardner, J. D., Bailey, L. J., Brunold, T. C., and Fox, B. G. (2007) Characterization of the nitrosyl adduct of substrate-bound mouse cysteine dioxygenase by electron paramagnetic resonance: Electronic structure of the active site and mechanistic implications. *Biochemistry 46*, 8569−8578.

(22) Souness, R. J., Kleffmann, T., Tchesnokov, E. P., Wilbanks, S. M., Jameson, G. B., and Jameson, G. N. (2013) Mechanistic implications of persulfenate and persulfide binding in the active site of cysteine dioxygenase. *Biochemistry 52*, 7606−7617.

(23) Leslie, A. W., and Powell, H. (2007) Processing diffraction data with mosflm. In *Evolving Methods for Macromolecular Crystallography* (Read, R., and Sussman, J., Eds.) pp 41−51, Springer, Dordrecht, The Netherlands.

(24) Evans, P. R., and Murshudov, G. N. (2013) How good are my data and what is the resolution? *Acta Crystallogr. D69*, 1204−1214.

(25) Karplus, P. A., and Diederichs, K. (2012) Linking crystallographic model and data quality. *Science 336*, 1030−1033.

(26) Adams, P. D., Afonine, P. V., Bunkoczi, G., Chen, V. B., Davis, I. W., Echols, N., Headd, J. J., Hung, L. W., Kapral, G. J., Grosse-Kunstleve, R. W., McCoy, A. J., Moriarty, N. W., Oeffner, R., Read, R. J., Richardson, D. C., Richardson, J. S., Terwilliger, T. C., and Zwart, P. H. (2010) PHENIX: A comprehensive Python-based system for macromolecular structure solution. *Acta Crystallogr. D66*, 213−221.

(27) Emsley, P., and Cowtan, K. (2004) Coot: Model-building tools for molecular graphics. *Acta Crystallogr. D60*, 2126−2132.

(28) Painter, J., and Merritt, E. A. (2006) Optimal description of a protein structure in terms of multiple groups undergoing TLS motion. *Acta Crystallogr. D62*, 439−450.

(29) Painter, J., and Merritt, E. A. (2006) TLSMD web server for the generation of multi-group TLS models. *J. Appl. Crystallogr. 39*, 109−111.

(30) Hethey, J., Lai, J., Loutet, S., Martin, M., and Tang, V. (2002) Effects of tricine, glycine and Tris buffers on alkaline phosphatase activity. *Journal of Experimental Microbiology and Immunology 2*, 33−38.

(31) Fellner, M., Doughty, L. M., Jameson, G. N. L., and Wilbanks, S. M. (2014) A chromogenic assay of substrate depletion by thiol dioxygenases. *Anal. Biochem. 459*, 56−60.

(32) Alberty, R. A., and Massey, V. (1954) On the interpretation of the pH variation of the maximum initial velocity of an enzyme-catalyzed reaction. *Biochim. Biophys. Acta 13*, 347−353.

(33) Waley, S. G. (1953) Some aspects of the kinetics of enzymic reactions. *Biochim. Biophys. Acta 10*, 27−34.

(34) Cornish-Bowden, A. (2013) *Fundamentals of enzyme kinetics*, John Wiley & Sons, New York.

(35) Eisenthal, R., Danson, M. J., and Hough, D. W. (2007) Catalytic efficiency and k_{cat}/K_M: A useful comparator? *Trends Biotechnol. 25*, 247−249.

(36) Albery, W. J., and Knowles, J. R. (1976) Evolution of enzyme function and the development of catalytic efficiency. *Biochemistry 15*, 5631−5640.
(37) Carrillo, N., and Ceccarelli, E. A. (2003) Open questions in ferredoxin-NADP$^+$ reductase catalytic mechanism. *Eur. J. Biochem. 270*, 1900−1915.
(38) Fersht, A. (1999) *Structure and Mechanism in Protein Science: A Guide to Enzyme Catalysis and Protein Folding*, W. H. Freeman and Co., New York.
(39) Ceccarelli, E. A., Carrillo, N., and Roveri, O. A. (2008) Efficiency function for comparing catalytic competence. *Trends Biotechnol. 26*, 117−118.
(40) Pettersen, E. F., Goddard, T. D., Huang, C. C., Couch, G. S., Greenblatt, D. M., Meng, E. C., and Ferrin, T. E. (2004) UCSF Chimera: A visualization system for exploratory research and analysis. *J. Comput. Chem. 25*, 1605−1612.
(41) Siakkou, E., Wilbanks, S. M., and Jameson, G. N. L. (2010) Simplified cysteine dioxygenase activity assay allows simultaneous quantitation of both substrate and product. *Anal. Biochem. 405*, 127−131.
(42) Simmons, C. R., Hirschberger, L. L., Machi, M. S., and Stipanuk, M. H. (2006) Expression, purification, and kinetic characterization of recombinant rat cysteine dioxygenase, a non-heme metalloenzyme necessary for regulation of cellular cysteine levels. *Protein Expression Purif. 47*, 74−81.
(43) Chai, S. C., Jerkins, A. A., Banik, J. J., Shalev, I., Pinkham, J. L., Uden, P. C., and Maroney, M. J. (2005) Heterologous Expression, Purification, and Characterization of Recombinant Rat Cysteine Dioxygenase. *J. Biol. Chem. 280*, 9865−9869.
(44) Bagley, P. J., Hirschberger, L. L., and Stipanuk, M. H. (1995) Evaluation and Modification of an Assay Procedure for Cysteine Dioxygenase Activity: High-Performance Liquid Chromatography Method for Measurement of Cysteine Sulfinate and Demonstration of Physiological Relevance of Cysteine Dioxygenase Activity in Cysteine Catabolism. *Anal. Biochem. 227*, 40−48.
(45) Misra, C. H., and Olney, J. W. (1975) Cysteine oxidase in brain. *Brain Res. 97*, 117−126.
(46) Ewetz, L., and Sörbo, B. (1966) Characteristics of the cysteinesulfinate-forming enzyme system in rat liver. *Biochim. Biophys. Acta 128*, 296−305.
(47) Wainer, A. (1965) The production of cysteinesulfinic acid from cysteine in vitro. *Biochim. Biophys. Acta 104*, 405−412.
(48) Kumar, V., Maresca, B., Sacco, M., Goewert, R., Kobayashi, G. S., and Medoff, G. (1983) Purification and characterization of a cysteine dioxygenase from the yeast phase of *Histoplasma capsulatum*. *Biochemistry 22*, 762−768.
(49) Sakakibara, S., Yamaguchi, K., Hosokawa, Y., Kohashi, N., Ueda, I., and Sakamoto, Y. (1976) Purification and some properties of rat liver cysteine oxidase (cysteine dioxygenase). *Biochim. Biophys. Acta 422*, 273−279.